

# Characterization of DNA Probes Immobilized on Gold Surfaces

Tonya M. Herne\* and Michael J. Tarlov

Contribution from the Chemical Science and Technology Laboratory,  
National Institute of Standards and Technology, Gaithersburg, Maryland 20899-0001

Received June 13, 1997<sup>⊗</sup>

**Abstract:** We have characterized thiol-derivatized, single-stranded DNA (5'-HS-(CH<sub>2</sub>)<sub>6</sub>-CAC GAC GTT GTA AAA CGA CGG CCA G-3', abbreviated HS-ssDNA) attached to gold via a sulfur-gold linkage using X-ray photoelectron spectroscopy (XPS), ellipsometry, and <sup>32</sup>P-radiolabeling experiments. We found that hybridization of surface-bound HS-ssDNA is dependent on surface coverage. The buffer concentration of the HS-ssDNA solution was found to have a profound effect on surface coverage, with adsorption greatly reduced at low salt concentration. More precise control over surface coverage was achieved by creating mixed monolayers of the thiol-derivatized probe and a spacer thiol, mercaptohexanol (MCH), by way of a two-step method, where first the gold substrate is exposed to a micromolar solution of HS-ssDNA, followed by exposure to a millimolar solution of MCH. A primary advantage of using this two-step process to form HS-ssDNA/MCH mixed monolayers is that nonspecifically adsorbed DNA is largely removed from the surface. Thus, the majority of surface-bound probes are accessible for specific hybridization with complementary oligonucleotides and are able to discriminate between complementary and noncomplementary target molecules. Moreover, the probe-modified surfaces were found to be stable, and hybridization reactions were found to be completely reversible and specific in a series of experiments where duplex melting was examined.

## Introduction

Surface-confined DNA probe arrays are important in the development of novel DNA sequencing and gene mapping technologies.<sup>1–11</sup> A typical array-based sensor consists of single-stranded oligonucleotides of different sequences, called probes, attached to a surface, with the identity and location of each surface-bound DNA probe known. Miniaturized probe arrays have been fabricated containing up to 135 000 probes with specific sequences confined to areas of 35 × 35 μm<sup>2</sup> or less.<sup>9</sup> The array is exposed to a fluorescently labeled or radio-labeled single strand of DNA of unknown sequence, a target, that binds or hybridizes to complementary probes in the array. Hybridization reactions of the tagged strands are then detected using a fluorescence or radioimaging technique, the array locations of the tagged strands are determined, and the sequence of the unknown strand is deduced.

While DNA array-based technologies hold great promise for rapid and accurate sequence determination and diagnosis of genetic diseases, surprisingly little is known about the surface

structures of bound probes and the impact of the surface on hybridization reactions. It is interesting to note that, in spite of the tremendous potential held by these new DNA technologies, little has been done in the way of physical characterization of the surface species. For example, the structure-function relationships of the immobilized probes on the surface have not been examined in great detail, nor has the role of probe coverage on hybridization efficiency been rigorously examined.

In this paper, we describe the use of alkanethiol self-assembly methods to fabricate DNA probe-modified gold surfaces with known and reproducible probe coverages that exhibit high hybridization activity. In our approach, we precisely control the surface coverage of thiol-derivatized DNA on the surface by forming mixed monolayers of the thiol-derivatized probe and a spacer thiol, 6-mercapto-1-hexanol (MCH). The spacer thiol was carefully chosen to minimize nonspecific adsorption of single-stranded DNA. Other investigators have employed thiol-derivatized, single-stranded DNA to study hybridization reactions on surfaces; however, the effect of probe coverage on hybridization reactions was not examined in great detail.<sup>6,12–14</sup> In this report, the two-component DNA/MCH monolayers are thoroughly characterized using X-ray photoelectron spectroscopy (XPS), ellipsometry, and <sup>32</sup>P-radiolabeling experiments. In addition to studying the effect of probe coverage on hybridization, the melt behavior of the surface-bound duplex has been examined, and the temperature stability of the surface-bound DNA was explored.

## Experimental Section

Single-crystal (100) silicon wafers were used as substrates in the preparation of evaporated Au films. The silicon wafers were cut into

<sup>⊗</sup> Abstract published in *Advance ACS Abstracts*, September 1, 1997.

(1) Maskos, U.; Southern, E. M. *Nucleic Acids Res.* **1993**, *21*, 4663–4669.

(2) Maskos, U.; Southern, E. M. *Nucleic Acids Res.* **1992**, *20*, 1679–1684.

(3) Maskos, U.; Southern, E. M. *Nucleic Acids Res.* **1992**, *20*, 1675–1678.

(4) Southern, E. M.; Case-Green, S. C.; Elder, J. K.; Johnson, M.; Mir, K. U.; Wang, L.; Williams, J. C. *Nucleic Acids Res.* **1994**, *22*, 1368–1373.

(5) Chrisey, L. A.; Robets, P. M.; Benezra, V. I.; Dressick, W. J.; Dulcey, C. S.; Calvert, J. M. *Mater. Res. Soc. Sym. Proc.* **1994**, *330*, 179.

(6) Lee, G. U.; Chrisey, L. A.; Colton, R. J. *Science* **1994**, *266*, 771–773.

(7) Nikiforov, T. T.; Rendle, R. B.; Goelet, P.; Rogers, Y.-H.; Kotewicz, M. L.; Anderson, A.; Trainor, G. L.; Knapp, M. R. *Nucleic Acids Res.* **1994**, *22*, 4167–4175.

(8) Lamture, J. B.; Beattie, K. L.; Burke, B. E.; Eggers, M. D.; Ehrlich, D. J.; Fowler, R.; Hollis, M. A.; Kosicki, B. B.; Reich, R. K.; Smith, S. R.; Varma, R. S.; Hogan, M. E. *Nucleic Acids Res.* **1994**, *22*, 2121–2125.

(9) Chee, M.; Yang, R.; Hubbell, E.; Berno, A.; Huang, X. C.; Stern, D.; Winkler, J.; Lockhart, D. J.; Morris, M. S.; Fodor, S. P. A. *Science* **1996**, *274*, 610–614.

(10) Pease, A. C.; Solas, D.; Sullivan, E. J.; Cronin, M. T.; Holmes, C. P.; Fodor, S. P. A. *Proc. Natl. Acad. Sci. U.S.A.* **1994**, *91*, 5022–5026.

(11) Chan, V.; Graves, D. J.; McKenzie, S. E. *Biophys. J.* **1995**, *69*, 2243–2255.

(12) Okahata, Y.; Matsunobu, Y.; Ijio, K.; Mukae, M.; Murakami, A.; Makino, K. *J. Am. Chem. Soc.* **1992**, *114*, 8299–8300.

(13) Leavitt, A. J.; Wenzler, L. A.; Williams, J. M.; Beebe, T. P. *J. Phys. Chem.* **1994**, *98*, 8742–8746.

(14) Rabke-Clemmer, C. E.; Leavitt, A. J.; Beebe, T. P. *Langmuir* **1994**, *10*, 1796–1800.

(15) Tarlov, M. J. *Langmuir* **1992**, *8*, 80–90.

pieces (ca.  $1.3 \times 1.5 \text{ cm}^2$  for XPS and ellipsometry,  $0.3 \times 1.3 \text{ cm}^2$  for the radiolabeling experiments) and cleaned by sequential sonication for 15 min each in dichloromethane, methanol, and Millipore deionized water.<sup>16</sup> The silicon pieces were dipped in 10% HF immediately before Au film deposition. The Au thin films were prepared by thermal evaporation of 200 nm of Au onto a 10 nm Cr adhesion layer. The Au substrates were cleaned in piranha solution (70%  $\text{H}_2\text{SO}_4$ :30%  $\text{H}_2\text{O}_2$ ) before exposure to the sample solutions. [CAUTION: Piranha solution can react violently with organic materials, and should be handled with extreme caution. Piranha solution should not be stored in tightly sealed containers.]

The DNA used in this study was synthesized by standard phosphoramidite chemistry and was generously provided by Joel Hoskins (National Institutes of Health, Bethesda, MD). The thiolated single-stranded DNA, abbreviated HS-ssDNA, is a 25-base oligonucleotide with the following sequence: 5'-HS-( $\text{CH}_2$ )<sub>6</sub>-CAC GAC GTT GTA AAA CGA CGG CCA G-3'. The complementary single-stranded DNA, abbreviated ssDNA-C, is a 25-mer with the following sequence: 5'-CTG GCC GTC GTT TTA CAA CGT CGT G-3'. The non-complementary control has the same sequence as the immobilized probe without the HS-( $\text{CH}_2$ )<sub>6</sub>- attachment at the 5' end. The mercaptohexanol was generously donated by Professor Cary Miller at the University of Maryland, College Park, MD.

The HS-ssDNA surfaces were prepared by placing piranha-cleaned Au in 1.0 M  $\text{KH}_2\text{PO}_4$  buffer solutions of DNA (pH 3.8), unless otherwise stated. Mixed monolayer surfaces containing HS-ssDNA and MCH were prepared by immersing the clean gold substrate in a 1.0  $\mu\text{M}$  solution of HS-ssDNA for a specific amount of time, followed by a 1 h exposure of the sample to an aqueous solution of 1.0 mM MCH. Before analysis or hybridization, each sample was rinsed thoroughly with deionized water.

Hybridization activity of the HS-ssDNA immobilized on gold was determined using <sup>32</sup>P radiolabeling. Complementary and noncomplementary DNA oligonucleotides were radiolabeled with <sup>32</sup>P using T4 polynucleotide kinase and  $\gamma$  <sup>32</sup>P ATP (3000 Ci/mmol) from New England Nuclear (Boston, MA).<sup>16</sup> Hybridization was performed at 24 °C for 90 min in TE -1 M NaCl (10 mM Tris-HCl, 1 mM EDTA, 1 M NaCl). After hybridization, samples were rinsed in 1 mL of TE eight times, ten seconds each rinse. Samples were air-dried before imaging. Hybridization of the surface-bound probe with its complement was monitored by obtaining radioimages with the Fuji Bio-Imaging Analyzer Model BAS 2000.<sup>16</sup> The spatial resolution of this imaging instrument is 100  $\mu\text{m}$ .

XPS spectra were obtained with the surface analysis system described in ref 15. An Al anode operated at 240 W was used to generate X-rays. A hemispherical analyzer was operated at a band pass energy of 100 eV, with the entrance aperture aligned with the surface normal. Ellipsometric data were obtained on a Rudolph Research ellipsometer (model 43603-200E) equipped with a He-Ne laser.<sup>16</sup> The angle of incidence was 70° from the surface normal, the beam spot size was approximately 2 mm<sup>2</sup>, and the refractive index ( $\eta$ ) of the adsorbed thiolated DNA was assumed to be 1.45. Thickness values were obtained by averaging three measurements per sample.

## Results and Discussion

Ideally, the thiol-derivatized DNA molecules interact with the surface exclusively through the sulfur atom of the thiol group. It is possible, however, that the nitrogen-containing nucleotide side chains interact directly with the surface. To determine whether HS-ssDNA is adsorbed "specifically" through the sulfur atom or "nonspecifically" through the nucleotide bases, or some other functionality of the DNA, XPS data from the thiol-derivatized DNA (HS-ssDNA) and the non-thiol derivatized DNA (ssDNA) were obtained and compared. We have found that the presence of the N 1s peak in the XPS data is a reliable indication that DNA is adsorbed on the surface. Bare gold samples exposed to buffer solutions containing no

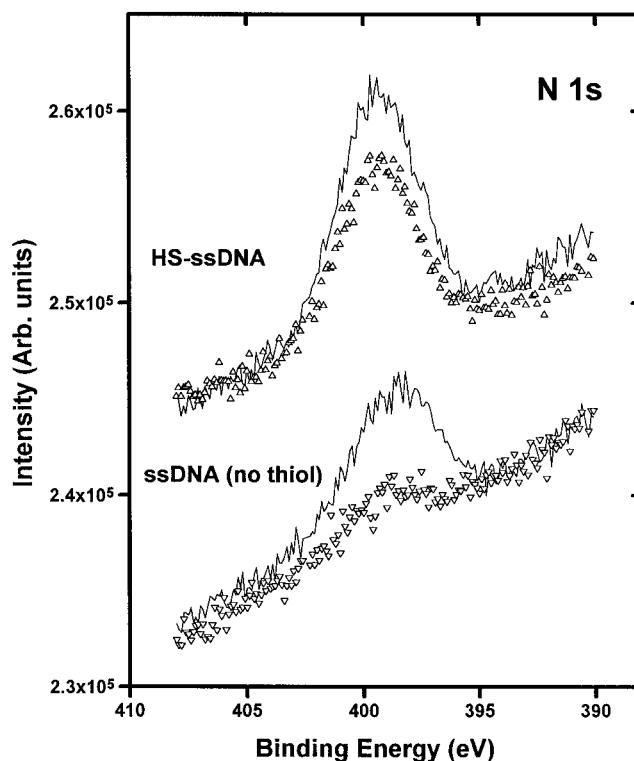


**Figure 1.** XPS N 1s spectra of thiol-derivatized and non-thiol-derivatized ssDNA before (solid lines) and after (triangles) exposure to MCH. Posttreatment with MCH results in displacement of nearly all of the non-thiol-derivatized DNA, but only a small amount of the surface-bound HS-ssDNA.

DNA exhibit no XPS-detectable nitrogen; we therefore conclude that any observed N 1s signal originates exclusively from the nitrogen-containing purine and pyrimidine bases of DNA. Furthermore, the relative amounts of adsorbed DNA for different samples can be determined by comparison of N 1s peak areas.

The XPS N 1s data for HS-ssDNA and the ssDNA are shown in Figure 1. The N 1s peak area of the non-thiol-derivatized DNA is approximately 50 to 60% of that measured for adsorbed HS-ssDNA, indicating that more ssDNA is adsorbed when the ssDNA molecule is derivatized with the thiol functionality. The higher intensity of the N 1s signal for HS-ssDNA is evidence that the strong thiol-gold interaction drives the adsorption of HS-ssDNA to higher coverages, compared to the non-thiolated DNA. There is a significant amount of DNA adsorption for the nonderivatized oligonucleotide, however, suggesting that ssDNA will interact with and adsorb on the surface when no thiol group is present. It is interesting to note that the nonderivatized DNA is adsorbed strongly on the surface; it is not removed by extensive rinsing with buffer or water, or heating the gold surface to 75 °C. On the basis of the presence of the non-thiol-derivatized DNA on the surface, the possibility of interaction of purine and pyrimidine bases with gold surfaces cannot be ruled out. We speculate that the nucleotide side chains play a role in the adsorption of DNA, and at least initially, the nucleotide side chains may be interacting directly with the surface. That is, the molecule may adsorb on the surface first through the nitrogen-containing bases, and then may reorganize on the surface, with the thiol group becoming the primary or most important point of attachment.

Ellipsometry was used to determine an equivalent thickness for the HS-ssDNA film on gold. In calculating thickness values, a simple model is assumed of uniform film thickness and refractive index ( $\eta = 1.45$ ). Ellipsometry on the HS-ssDNA film in air gives a HS-ssDNA film thickness of  $33 \pm 2 \text{ \AA}$ . If the DNA 25-mer molecules were adsorbed on the gold

(16) Certain commercial products and instruments are identified to adequately specify the experimental procedure. In no case does such identification imply endorsement by the National Institute of Standards and Technology.

through the thiol functionality and stretched to full length, we would expect an equivalent film thickness of greater than 160 Å,<sup>17</sup> approximately 5 times the measured value. Because the ellipsometric data give a HS-ssDNA film thickness of approximately 20% of the expected maximum thickness, we conclude that the HS-ssDNA monolayer is not a tightly packed monolayer, and that the DNA chains are not oriented perpendicular to the surface.

As a means of measuring how strongly bound the HS-ssDNA and non-thiolated ssDNA molecules are to the surface, a series of displacement experiments were designed where both HS-ssDNA and ssDNA surfaces were exposed to an aqueous solution of 1 mM mercaptohexanol (MCH) for 1 h. The XPS N 1s data obtained after posttreatment with MCH for both HS-ssDNA and ssDNA samples are shown in the scatter plots in Figure 1, along with the XPS data obtained before MCH exposure. It is apparent that both HS-ssDNA and non-thiolated ssDNA coverages are altered by posttreatment with MCH. The N 1s peak obtained from the HS-ssDNA sample is slightly less intense than that observed before exposure to MCH, indicating that a small amount of HS-ssDNA has been removed or displaced from the surface. A more dramatic difference between the "before" and "after" XPS data for the non-thiolated ssDNA is observed. Nearly complete displacement of the non-thiolated DNA occurs after exposure to MCH. The significance of these experiments is 3-fold. First, it is clear that the HS-ssDNA molecule is adsorbed through the sulfur atom, as the HS-ssDNA is not displaced by MCH posttreatment, in contrast to what was observed for the non-thiolated ssDNA. Second, posttreatment with MCH results in removal of nonspecifically bound, single-stranded DNA. Third, we infer that the majority of the HS-ssDNA molecules are anchored to the surface through the sulfur group. In effect, the HS-ssDNA molecules are raised off the surface by MCH posttreatment to a surface conformation where they are bound solely by the sulfur atom.

The role of buffer concentration (in this case,  $\text{KH}_2\text{PO}_4$ ) and its influence on adsorption of HS-ssDNA on gold were also explored. Shown in Figure 2 are XPS data obtained from samples immersed in 1.0  $\mu\text{M}$  HS-ssDNA solutions, prepared either in pure water or in 1.0 M  $\text{KH}_2\text{PO}_4$  buffer. For the HS-ssDNA solution prepared in pure water, essentially no N 1s peak is observed, indicating that HS-ssDNA dissolved in water does not adsorb on gold. In contrast, a relatively intense N 1s peak is observed when a sample is exposed to a 1.0  $\mu\text{M}$  solution of HS-ssDNA prepared in 1.0 M  $\text{KH}_2\text{PO}_4$  buffer. To explore further the role of buffer concentration on adsorption of HS-ssDNA, XPS data from a series of samples exposed to 1.0  $\mu\text{M}$  HS-ssDNA solutions prepared in different concentrations of  $\text{KH}_2\text{PO}_4$  buffer were obtained. The normalized N 1s peak areas obtained from this series of samples are plotted as a function of  $\text{KH}_2\text{PO}_4$  concentration in Figure 3. The XPS N 1s peak area for buffer concentrations of  $2.7 \times 10^{-4}$  to 1.0 M  $\text{KH}_2\text{PO}_4$  grows 5-fold as the buffer concentration is increased, evidence that the buffer concentration plays a critical role in adsorption of DNA. The data suggest that maximum HS-ssDNA coverage is achieved when the  $\text{KH}_2\text{PO}_4$  concentration is greater than 0.4 M. The importance of ionic strength in determining surface coverage of DNA is not surprising, given that HS-ssDNA is a negatively charged molecule with 25 ionizable phosphate groups. We postulate that intermolecular electrostatic repulsion between neighboring strands of DNA is minimized under the high ionic strength conditions, as the charged strands are better electrostatically shielded, thus allowing higher surface coverages of HS-ssDNA.

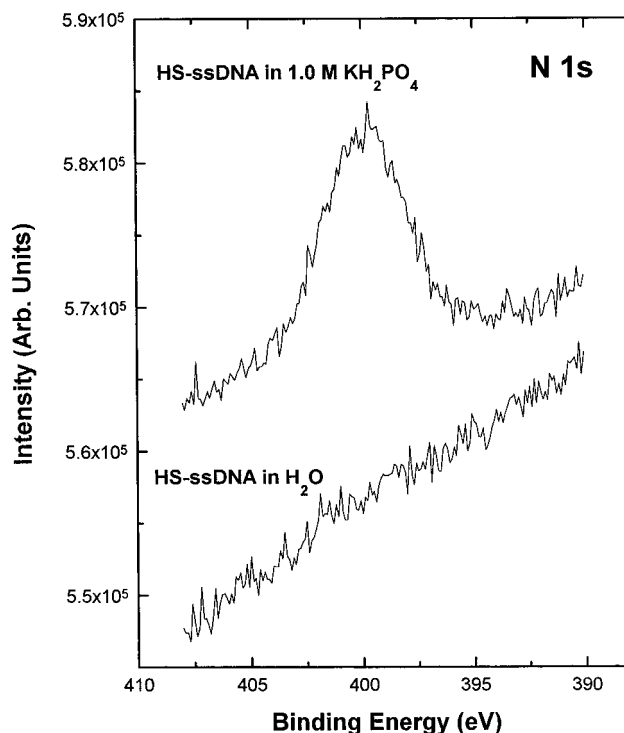


**Figure 2.** XPS N 1s data obtained from 1.0  $\mu\text{M}$  HS-ssDNA in pure water and in 1.0 M  $\text{KH}_2\text{PO}_4$ . No HS-ssDNA adsorbs on the surface from an aqueous solution of HS-ssDNA when no buffer is present.

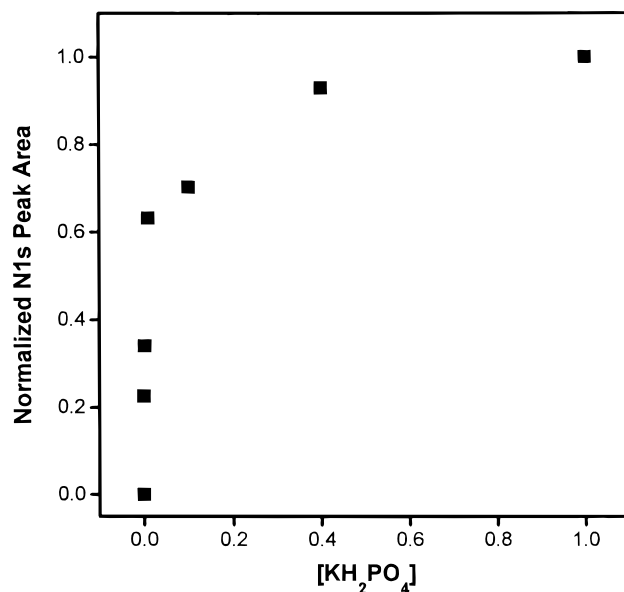


**Figure 3.** Normalized XPS N 1s peak areas plotted as a function of buffer concentration of the 1.0  $\mu\text{M}$  HS-ssDNA solution.

Hybridization activity of the sample with the highest HS-ssDNA coverage was investigated by exposing the sample to its radiolabeled complement. No signal from the radiolabel was measured, indicating that hybridization did not occur. We conclude that hybridization on this surface is inhibited due to steric and electrostatic factors. The complement cannot access the surface-bound HS-ssDNA, as the molecules on the surface are too tightly packed. In addition, the dense packing of these charged phosphate groups likely electrostatically inhibits the approach and binding of the similarly charged complement.

To allow hybridization, a strategy was adopted to vary the coverage of surface-bound, single-stranded DNA by the formation of a two-component monolayer consisting of HS-ssDNA and a spacer thiol molecule, MCH. Schematics of the pure HS-ssDNA surface and the two-component surface are shown in

(17) Peterlinz, K. A.; Georgiadis, R. M.; Herne, T. M.; Tarlov, M. J. *J. Am. Chem. Soc.* **1997**, *119*, 3401–3402.

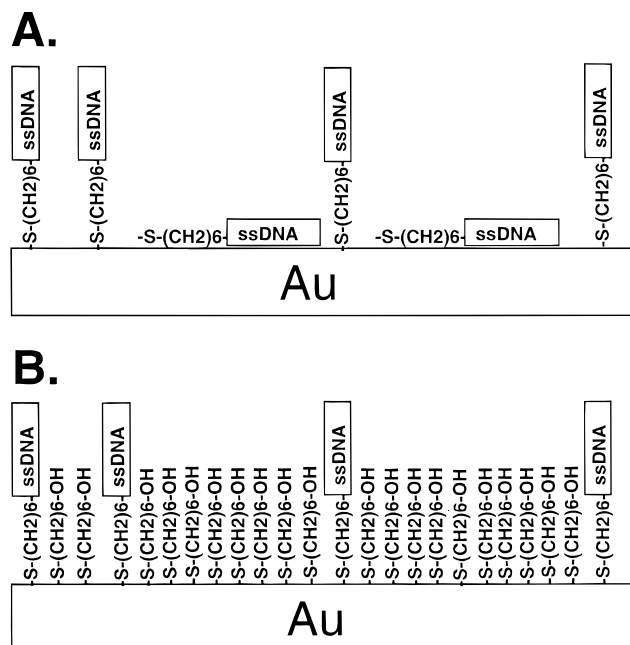


**Figure 4.** Schematic of (A) HS-ssDNA on Au and (B) both HS-ssDNA and MCH adsorbed on gold.

Figure 4, parts A and B. Before exposure to MCH, we speculate that the HS-ssDNA molecules interact with the surface through both the nitrogen-containing nucleotide bases and the sulfur atom of the thiol group. After exposure to MCH, we predict that the HS-ssDNA molecules are adsorbed on the surface through the sulfur atoms, and the nucleotide bases do not interact with the surface. MCH was selected as the spacer thiol for three reasons. First, it was determined by XPS that nonspecific binding of DNA on a SAM of MCH does not occur. That is, if we form a pure MCH monolayer, DNA will not adsorb on the hydroxy-terminated surface of the MCH monolayer.<sup>18</sup> Second, MCH is soluble in aqueous solutions. Third, the 6-carbon chain of MCH is the same length as the methylene group spacer in HS-ssDNA, and is not long enough to interfere with the hybridization reactions of surface-bound DNA.

Mixed HS-ssDNA/MCH monolayers of varying coverage were formed by a two-step process. First, clean bare gold was immersed in a 1.0  $\mu\text{M}$  HS-ssDNA solution in 1.0 M  $\text{KH}_2\text{PO}_4$  for a specific amount of time (referred to here as “exposure time”), followed by rinsing with water. Second, the HS-ssDNA-treated surface was placed in a solution of 1.0 mM MCH dissolved in pure water for 1 h. A series of HS-ssDNA/MCH surfaces were prepared by the above method, with exposure times ranging from 1 min to 21.9 h. The relative amount of HS-ssDNA on the surface was determined by measuring the XPS N 1s peak areas. The normalized N 1s peak areas plotted as a function of time in the HS-ssDNA solution are shown in Figure 5. The N 1s peak intensity increases with exposure time, indicating a direct correlation between the amount of DNA on the surface and the exposure time. The amount of HS-ssDNA appears to reach a maximum at 240 min, with further exposure resulting in little additional adsorption. This result is qualitatively consistent with the monolayer formation kinetics observed in surface plasmon resonance spectroscopic studies.<sup>17</sup>

To assess the optimal coverage for hybridization, a series of surfaces with varying HS-ssDNA coverages were exposed to separate hybridization solutions containing the radiolabeled complement for 90 min, and then rinsed with TE buffer.

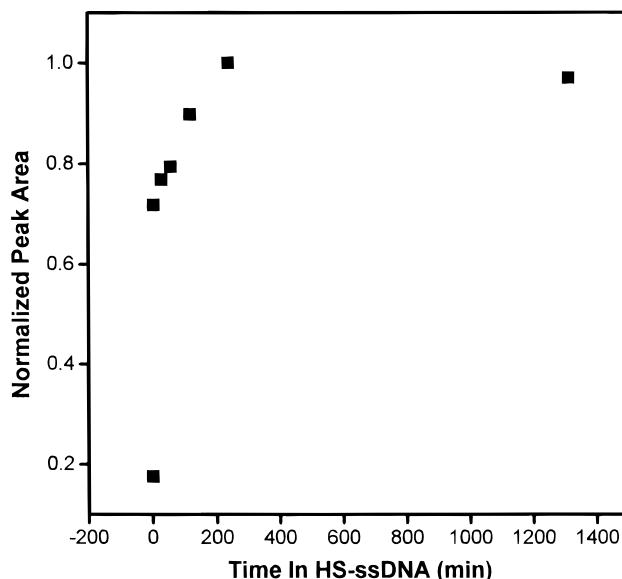


**Figure 5.** Normalized N 1s peak areas plotted as a function of sample exposure time to HS-ssDNA. The amount of HS-ssDNA on the surface can be controlled by varying the exposure time.

**Table 1.** Data Obtained from Radioimages of HS-ssDNA/MCH Monolayers Exposed to  $^{32}\text{P}$ -Radiolabeled Complement

sample	time in HS-ssDNA (min)	time in MCH (min)	intensity <sup>a</sup> (counts/cm <sup>2</sup> )	<sup>32</sup> P-radiolabeled DNA <sup>b</sup> (molecules/cm <sup>2</sup> )
bare Au	0.0	0.0	6836 ± 83	3.1 (±0.03) × 10 <sup>12</sup>
1 <sup>c</sup>	0.0	60	64 ± 8	2.9 (±0.4) × 10 <sup>10</sup>
2	0.25	60	773 ± 28	3.5 (±0.1) × 10 <sup>11</sup>
3	1.0	60	4018 ± 64	1.8 (±0.03) × 10 <sup>12</sup>
4	5.0	60	8818 ± 94	4.0 (±0.04) × 10 <sup>12</sup>
5	10.0	60	7064 ± 84	3.2 (±0.04) × 10 <sup>12</sup>
6	32.5	60	7627 ± 87	3.4 (±0.04) × 10 <sup>12</sup>
7	60.0	60	8491 ± 92	3.8 (±0.04) × 10 <sup>12</sup>
8	120.0	60	12627 ± 112	5.7 (±0.05) × 10 <sup>12</sup>
9	240.0	60	11418 ± 107	5.2 (±0.04) × 10 <sup>12</sup>
10	1313.0	60	9764 ± 99	4.4 (±0.04) × 10 <sup>12</sup>

<sup>a</sup> The intensity is obtained by totaling the number of counts in a circle of area 0.11 cm<sup>2</sup>. <sup>b</sup> Calculated by comparing the number of photostimulated luminescence counts measured on the gold substrates to a radioimage obtained of a spot of  $^{32}\text{P}$  radiolabeled DNA of known concentration. <sup>c</sup> MCH control sample.

Summarized in Table 1 are results from this set of experiments, along with results obtained from exposing a bare gold substrate and a pure MCH monolayer to solutions containing the  $^{32}\text{P}$ -radiolabeled complement. The bare gold and pure MCH samples serve as controls which monitor nonspecific adsorption of the radiolabeled target. In addition, a second set of identically prepared surfaces was exposed to a different radiolabeled oligonucleotide that was not complementary to the surface-bound probe. This set of samples was used to measure nonspecific binding of the radiolabeled probe to the surface as well as nonspecific hybridization between mismatched oligonucleotides.

Hybridization or adsorption of the  $^{32}\text{P}$ -radiolabeled complement to HS-ssDNA-coated substrates and the control samples appeared to be uniform in the radioimages. That is, bare patches or clumping of the radiolabeled oligonucleotides on the surface was not observed down to a level of 100  $\mu\text{m}$ , the lateral resolution of the imaging plate. The pure MCH sample, sample 1 in Table 1, had very little of the radiolabeled target molecule bound to it. This result is consistent with our XPS studies, in which we found that HS-ssDNA and the non-thiol-derivatized DNA will not adsorb on MCH SAMs. In contrast, the bare gold substrate exhibited a significant amount of adsorbed radiolabeled complement. This is not surprising, given that we

(18) Herne, T. M.; Tarlov, M. J. We have determined, using XPS and  $^{32}\text{P}$  radiolabeling techniques, that ssDNA molecules will not adsorb on MCH SAMs (unpublished results).

have observed nonspecific adsorption of non-thiol-derivatized oligonucleotides on gold using XPS (see Figure 1). For the HS-ssDNA/MCH-coated surfaces, hybridization was evidenced by the binding of the radiolabeled probe to the substrate. As the HS-ssDNA coverage increases, the amount of radiolabeled probe on the surface is observed to increase, reach a maximum, and then decrease. The greatest number of hybridization events occurs on sample 8, which corresponds to an exposure time of 120 min. At higher HS-ssDNA coverages (exposure times > 120 min), we observe a decrease in the number of hybridization events. We attribute the decrease in the number of duplexes formed on the surface for higher coverage samples (samples 9 and 10) to steric and electrostatic hindrances arising from the more tightly packed DNA monolayer, as described earlier.

It is clear from the hybridization experiments that the optimal surface coverage for maximizing the number of hybridization events is that obtained for the 120 min HS-ssDNA exposure sample. For this work, we define the hybridization efficiency as the percentage of surface-bound probes undergoing hybridization with the radiolabeled target. The coverage of surface-bound probes in a similarly prepared HS-ssDNA/MCH mixed monolayer before hybridization was measured by SPR to be  $5.2 (\pm 0.8) \times 10^{12}$  molecules/cm<sup>2</sup>.<sup>17</sup> To estimate the hybridization efficiency on this surface, a known volume and concentration of radiolabeled DNA was spotted on filter paper and exposed to the imaging plate, from which the number of <sup>32</sup>P-labeled molecules/radioactive count was obtained. This number was then used to determine the number of radioactive target molecules/cm<sup>2</sup> that are either hybridized or adsorbed on the surface. For sample 8, we calculate that  $5.7 (\pm 0.05) \times 10^{12}$  molecules/cm<sup>2</sup> of the <sup>32</sup>P radiolabeled probe are present on the surface. The hybridization efficiency of the HS-ssDNA/MCH monolayer on sample 8 is then estimated to be ca. 100%. In surface plasmon resonance (SPR) spectroscopic studies of the HS-ssDNA/MCH two-component monolayers, hybridization efficiencies as high as 60–80% are reported.<sup>19</sup> The different hybridization efficiencies calculated here and in the SPR work are most likely a result of slight differences in sample preparation.<sup>19</sup> We note that the hybridization efficiency values obtained for the HS-ssDNA/MCH two component monolayer are much higher than have been reported for other surface-bound DNA systems. For example, for the two surface-bound probes (ACTG)<sub>5</sub> and C<sub>20</sub> on silica substrates, Lee et al. report that only 3.3% and 7.7% of the immobilized probes, respectively, are available for hybridization.<sup>6</sup> Maskos and Southern reported hybridization yields of 4 to 13% for oligonucleotides chemically bound to glass beads.<sup>2</sup> Finally, we add that a negligible amount of the noncomplementary <sup>32</sup>P-radiolabeled target adsorbed on the control set of identically prepared HS-ssDNA/MCH samples.

We have also investigated the melting behavior of the surface-bound duplexes and the reversibility of hybridization at the surface. DNA duplexes separate into single-stranded DNA, or unzip, at temperatures above  $T_m$ , the melt transition temperature. Upon heating the surface-bound duplex above  $T_m$ , we expect the duplex to melt, and the radiolabeled complement to diffuse from the surface, leaving behind the surface-bound HS-ssDNA. The original probe-covered surface should then be regenerated, and capable of hybridizing with complementary DNA again. For the 25-mer used in these studies, we estimate a solution  $T_m$  of 51 °C.<sup>20</sup> Two surfaces were prepared that had been exposed to HS-ssDNA for 1 h, followed by 1 h of posttreatment in MCH. Both surfaces were then exposed to the radiolabeled comple-

ment. Hybridization occurred as expected, as indicated by the presence of radioactivity from the hybridized complement on the surface in radioimages we obtained. The samples were then placed in TE buffer solution and heated to 70 °C, a temperature well above  $T_m$ . Nearly all of the radiolabeled complement is removed from the surface after the sample is heated to 70 °C, indicating melting of the duplexes. These two samples were then re-exposed to either the complementary or the noncomplementary radiolabeled probes. It was clear from the radioimages we obtained that the complementary ssDNA-C hybridized with the surface-bound HS-ssDNA (not shown). Furthermore, there was no measurable duplex formation or nonspecific binding of the radiolabeled noncomplement to the second substrate. There are two reasons for exposing the HS-ssDNA-coated surface to the noncomplementary probes. First, if the increase in temperature has resulted in desorption of HS-ssDNA or MCH from the surface during the melting experiment, the radiolabeled noncomplement may adsorb nonspecifically to the now bare spots on the gold surface. In this scenario, the resulting image will be "hotter", i.e. have more probe attached to the surface, than was observed for the sample exposed to noncomplementary DNA before the melt experiment. Second, we want to confirm that the surface-bound HS-ssDNA has not lost its specificity, and can still discriminate between complementary and noncomplementary sequences. We thus conclude that the HS-ssDNA/MCH system exhibits adequate temperature stability and good reversibility and selectivity for surface hybridization reactions.

## Conclusion

In summary, we have shown that thiol-derivatized, single-stranded DNA probes on gold surfaces are capable of hybridization with complementary DNA. From these experiments, we conclude that controlling the surface coverage of DNA is an important factor in maximizing hybridization efficiency. We have found that precise control over probe surface coverage can be achieved by creating mixed monolayers. Perhaps an even more important finding is that the DNA components in the mixed monolayers formed by our method are adsorbed on the surface primarily through the sulfur group, with few if any of the surface bound probes nonspecifically adsorbed on the surface. We believe that this attribute is responsible for the high hybridization efficiencies observed for the HS-ssDNA/MCH system. Other factors that may effect hybridization efficiency, such as the length of the methylene spacer between the thiol group and the DNA, are currently being studied. The effect of surface immobilization of the duplex on  $T_m$  is also being examined. The high hybridization efficiency measured for single-stranded DNA attached to gold with this mixed monolayer strategy is evidence that thiol-gold self-assembly methods may hold promise in constructing multicomponent DNA arrays.

**Acknowledgment.** The authors gratefully acknowledge the generous donation of mercaptohexanol from Professor Cary Miller at the University of Maryland and of the DNA used in this study from Joel Hoskins at the National Institutes of Health. We thank Dr. Keith H. McKenney (The Institute for Genomic Research, Rockville, MD) for his expert assistance in the radiolabeling experiments. We would also like to thank Dr. Stanley Abramowitz of the Advanced Technology Program at the National Institute of Standards and Technology for his support.

JA9719586

(19) The samples in the SPR experiment were prepared by forming the HS-ssDNA monolayer on gold over a period of 4–5 h, followed by a 14 h exposure to 1 μM MCH. The longer posttreatment in MCH may result in a less-than-optimized coverage of HS-ssDNA.

(20) From: Meinkoth, J.; Wahl, G. *Anal. Biochem.* **1984**, *138*, 267–284.  $T_m = 81.5 + 16.6(\log(\text{Na}^+)) + 0.41(\% \text{ G} + \text{C}) - 0.61(\% \text{ formamide present}) - 500/L$ , where  $L$  = the length of the shortest chain in the duplex.